Increasing Efficiency, Speed, and Responsivity of Vanadium Dioxide Based Photothermally Driven Actuators Using Single-Wall Carbon Nanotube Thin-Films

Tongyu Wang,[†] David Torres,[†] Félix E. Fernández,[‡] Andrew J. Green,[¶] Chuan Wang,[†] and Nelson Sepúlveda*,[†]

[†]Department of Electrical and Computer Engineering, Michigan State University, East Lansing, Michigan 48824,United States, [‡]Department of Physics, University of Puerto Rico—Mayaguez, Mayaguez, Puerto Rico 00681, United States, and [¶]Wyle Laboratories-Air Force Research Laboratories, Dayton, Ohio 45433, United States

ABSTRACT Vanadium dioxide (VO_2)-based actuators have demonstrated great performance in terms of strain energy density, speed, reversible actuation, programming capabilities, and large deflection. The relative low phase transition temperature of VO_2 (~68 °C) gives this technology an additional advantage over typical thermal actuators in terms of power consumption. However, this advantage can be further improved if light absorption is enhanced. Here we report a VO_2-based actuator technology that incorporates single-wall carbon nanotubes (SWNTs) as an effective light absorber to reduce the amount of photothermal energy required for actuation. It is demonstrated that the chemistry involved in the process of integrating the SWNT film with the VO_2-based actuators does not alter the quality of the VO_2 film, and that the addition of such film enhances the actuator performance in terms of speed and responsivity. More importantly, the results show that the combination of VO_2 and SWNT thin films is an effective approach to increase the photothermal efficiency of VO_2-based actuators. The integration of SWNT films in VO_2 devices can be easily applied to other VO_2-based phototransducers as well as to similar devices based on other phase-change materials. While adding a sufficiently thick layer of some arbitrary material with high absorption for the light used for actuation ($\lambda = 650$ nm wavelength in this case) could have improved conversion of light to heat in the device, it could also have impeded actuation by increasing its stiffness. It is noted, however, that the low effective Young's modulus of SWNT film coating used in this work does not impair the actuation range.

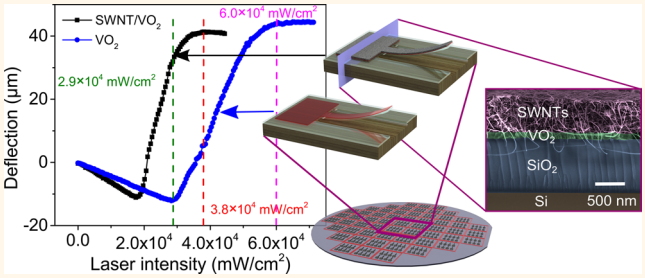

KEYWORDS: vanadium dioxide · carbon nanotubes · photoactuators · microactuators · thin films

VO_2 goes through a fully reversible solid-to-solid phase transformation, in which the crystal structure changes from a monoclinic phase to a tetragonal phase.[1−3] The phase change can be induced in multiple ways (*e.g.*, temperature,[1] ultrafast optical radiation,[4] mechanical stress,[5] and electric field[6]), resulting in abrupt change in the material's various properties.[1,3,7] The understanding of the underlying physics in the phase change of VO_2 has drawn the attention of scientists for over 50 years,[1,8−11] while the material's multifunctionality and fully reversible behavior has motivated applied scientists to integrate VO_2 in multiple devices, mainly in the past decade.[5,12−15] The promising applicability of VO_2 is further supported by the low temperature at which the phase change can be induced ($T \sim 68$ °C), which in fact makes it the material with the phase-change temperature closest to room temperature.[16]

Although the electrical and optical changes of VO_2 during the phase transition were reported about 50 years ago, it was not until 2010 when the effects of the stress changes in the film across the phase transition in micro structures were revealed.[12,13] It was reported that the change in area of the crystallographic planes in VO_2 parallel to

* Address correspondence to nelsons@egr.msu.edu.

Received for review February 6, 2015 and accepted April 8, 2015.

Published online April 08, 2015
10.1021/acsnano.5b00873

the surface of a micrometer-sized cantilever is capable of producing stress levels that generate significant actuation displacements and strain energy densities.[12,17,18] These results unveiled a new technology in micro transducers, where the actuation mechanism is based on the solid-to-solid phase-change of VO_2. Afterward, other research groups expanded the work to include VO_2 nanowires,[19,20] the use of the hysteretic behavior in VO_2 to program multiple mechanical[14,21,22] and optoelectronic states,[23] and the tuning of micromechanical resonators.[21,24]

In the field of microactuators, some of the advantages of thermal microactuators over their counterpart technologies (such as electrostatic[25] and piezoelectric actuators[26]) typically include large energy densities, low operating voltages, and large displacements.[27,28] However, before VO_2-based thermal actuators were reported, the most typical mechanism used in thermal actuators was the difference in thermal expansion coefficients between two layers forming a bimorph structure. To achieve large actuation of such devices, relatively large temperatures had to be reached. Nevertheless, high operating temperatures can result in permanent deformation, structural damage, and degradation in performance.[29,30] Furthermore, high actuation temperatures poses limitations on speed due to the long thermal constants (especially during cooling[24]). Phase-change actuation based on VO_2 represents a solution to this problem, by significantly lowering the actuation temperature to only ~68 °C. This lower actuation temperature was added to the multifunctionality aspect of VO_2 and large repeatable strain energy densities of VO_2-based actuators.[17]

Despite the advances made on exploiting VO_2's multifunctionality and low transition temperature in thermal actuators, little work has been done to increase the efficiency of VO_2-based actuators. One approach to reduce the required power for actuating VO_2 devices is to lower the transition temperature of the material. This has been previously achieved through doping (at the cost of a reduced magnitude in the material property changes across the transition)[31,32] or deposition of prestressed VO_2 film on specific substrates, such as single crystal TiO_2 (at the cost of a very expensive substrate and limitations during device fabrication).[33,34] In this paper, we present a simple and effective way of further improving the efficiency of photothermally actuated VO_2-based devices through the use of a SWNT thin film. The large optical absorption of SWNTs to visible and near-infrared wavelengths has been demonstrated to induce significant local heating for thermal micro actuators.[35] In this work, the high photothermal absorption of SWNTs for wavelengths in the visible range[36] is used to increase the efficiency, responsivity, and speed of VO_2-based devices that are actuated using visible (red) light. The experimental results show that the SWNT/VO_2-based actuators can provide the same deflection and speed as simple VO_2-based actuators, but use only approximately half the power. The improvement in the optical response indicates the potential application of the presented devices as VO_2-based photosensors. The successful integration of SWNTs with VO_2 films, without resulting in VO_2 film degradation was also demonstrated.

RESULTS AND DISCUSSION

Figure 1a schematically illustrates the fabrication process of the SWNT/VO_2-based cantilever actuator used in this work. The initial substrate was a 2-in. silicon wafer. A silicon dioxide (SiO_2) layer (1 μm thick) was first deposited by plasma-enhanced chemical vapor deposition (PECVD), followed by the deposition of a 120 nm thick VO_2 layer by the method of pulsed laser deposition (details in Methods section). The high quality of the VO_2 film is demonstrated by the more than 2 order drop in resistance observed when the temperature was increased from 30 to 100 °C (see Figure 1c). After VO_2 deposition, a SWNT thin film (~500 nm thick) made by vacuum filtration (details in the Methods section) was transferred on top of certain regions of the wafer. At this point, the substrate contains regions of $VO_2/SiO_2/Si$ and others of SWNT/$VO_2/SiO_2/Si$. This fabrication process guaranteed that the same VO_2 film was present in the final VO_2-based actuator devices (with and without a SWNT film coating), thus allowing for a fair device performance comparison. The SWNT film was patterned first using oxygen plasma, while the regions in the wafer where the VO_2 film was exposed were protected by photoresist. After patterning of the SWNT, the photoresist protecting the VO_2 layer was removed, and the same mask used for the SWNT was used to pattern the VO_2 layer using reactive ion etching CF_4-based recipe. A photoresist layer was also used to pattern the VO_2 film, and to protect it during the dicing of the wafer and the structure release using isotropic etching of silicon in XeF_2 gas. The photoresist was removed after release. The suspended structures showed initial bending at room temperature. This is due to the intrinsic thermal stress induced during the deposition of VO_2 at ~595 °C and subsequent cooling to room temperature. Figure 1d shows the optical transmittance spectra of VO_2 thin film (120 nm thick) on SiO_2 substrate, and the transmittance of the same sample, now coated with a SWNT film (800 nm thick). Top view microscope images of SWNT/VO_2- and VO_2-based cantilevers are shown in Figure 1b with a zoomed scanning electron microscope (SEM) image showing the cross section of SWNT/VO_2-based cantilever, in which display colors have been artificially modified for clarity.

Two main types of actuation experiments were performed: 1) conductive and, 2) photothermal heating actuation. The conductive heating experiments

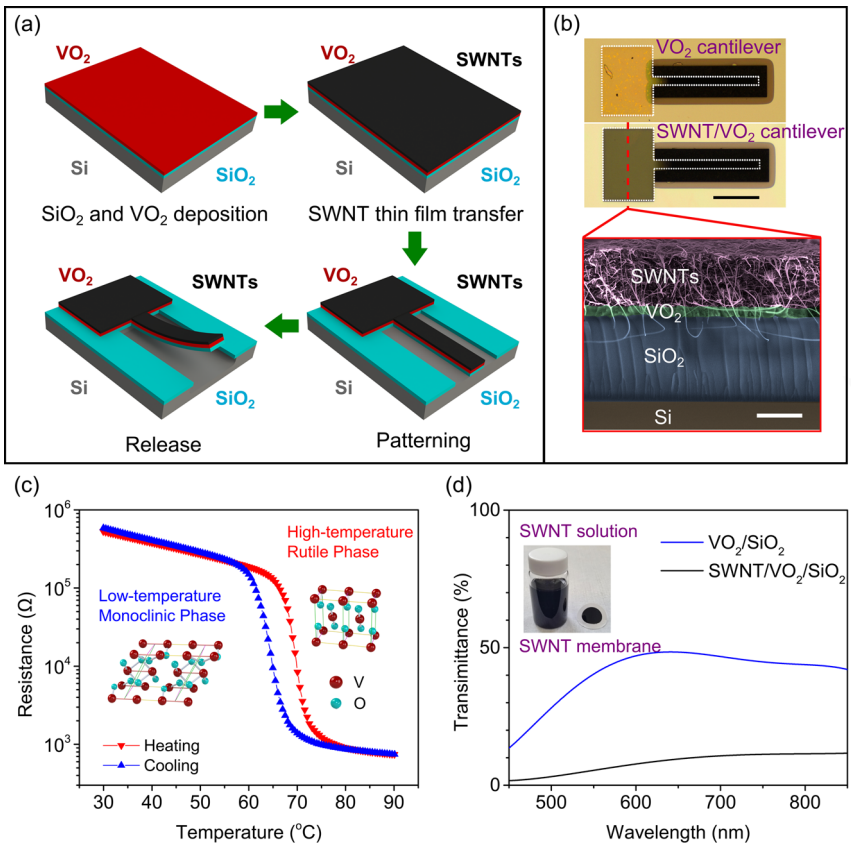

Figure 1. (a) Fabrication process of SWNT/VO_2-based cantilever actuator. For clarity, the bare VO_2-based devices are not shown. (b) Top view microscope images of SWNT/VO_2- and bare VO_2-based cantilevers with same length of 400 μm and width of 40 μm. The zoomed image is a SEM image of cross section of the SWNT/VO_2-based cantilever, in which colors have been artificially modified for clarity. The scale bars in the optical and SEM images are 200 μm and 500 nm, respectively. (c) Resistance of VO_2 as a function of temperature. (d) Measured optical transmittance spectra of VO_2 film (120 nm thick) over SiO_2 substrate before (blue curve) and after (black curve) being coated with SWNT film (800 nm thick).

were performed mainly to verify that the phase change characteristics of VO_2 film remain unchanged after the transfer of the SWNT film. The photothermal experiments demonstrated the larger efficiency, speed, and responsivity of SWNT/VO_2-based actuators. In the conductive heating experiments, only a Peltier heater was used, whereas in the photothermal experiments, the same Peltier heater was used only to provide a constant temperature offset while laser pulses were applied.

Actuation by Conductive Heating/Cooling. The actuator deflection is defined in this work as the displacement of cantilever's tip along the direction normal to initial bending. The deflection of SWNT/VO_2 and bare VO_2 cantilever actuators was studied as their temperature varied by using conductive heating through a Peltier heater under the chips (Figure 2a). This conductive heating produced a change in temperature that was nearly uniform in the entire chip substrate. The typical hysteretic shape of deflection curve of one heating and cooling cycle was obtained for both cantilever structures, which implies that the phase transition of VO_2 is the dominant mechanism that produces actuation for both devices. The effects of the mismatch between the thermal expansion coefficients of the SWNT and VO_2 layers is small during the phase transition, and the low Young's modulus of the SWNT film allows for minimal deflection differences between both devices. For regions outside the phase transition (*i.e.*, temperatures below 65 °C and above 80 °C) the observed bending in the opposite direction to the one during the phase transition is produced by the larger thermal expansion coefficients of SWNT and VO_2 films when compared to SiO_2 (see Table 1).

It can be noticed in Figure 2a that the maximum deflection for the SWNT/VO_2-based actuator is ~10 μm smaller than that of the bare VO_2-based one. This is probably due mainly to the larger thickness of the SWNT/VO_2 device, which increases the overall structure spring constant and bending resistance. However, the transition temperatures of both cantilevers are practically identical, which indicates that the quality of VO_2 remains unaltered after the SWNT thin film transfer.

The first part of the videos included in the Supporting Information show the deflection of both devices as the heater temperature is increased from 30 to 100 °C.

Actuation by Pulsed Optical Irradiation. The temperature of the substrate was maintained at 30 °C by

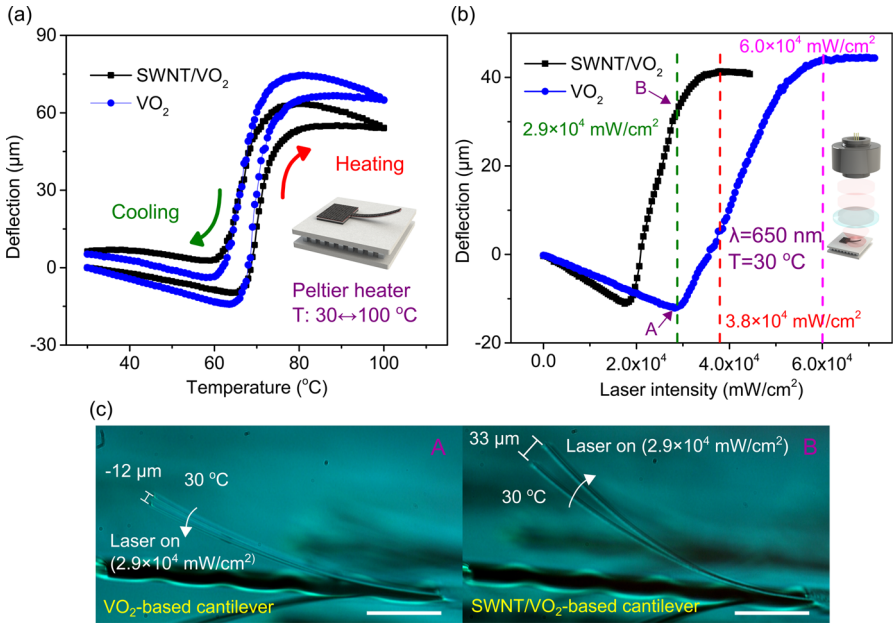

Figure 2. (a) Measured displacement of the VO_2 cantilevers and SWNT/VO_2-based cantilevers as functions of temperature (a) and intensity of laser pulses (b). In (a), the temperature is varied using a Peltier heater, while laser was turned off. In (b), the temperature was set to 30 °C, while laser pulses were applied by controlling the current of a laser diode. The intensities marked with the green and red dashed lines are the ones used in the time-response experiments. (c) Images of cantilevers corresponse to the laser intensities A and B labeled in (b). The scale bar is 100 μm.

TABLE 1. Materials Properties Used in the Finite Element Simulations and for Discussions of Results.[24,35,37−39]

materials	SiO_2	VO_2	SWNT film
density (kg m^{-3})	2200	4670	1500
Thermal conductivity (W m^{-1} K^{-1})	1.4	5	0.07
Heat capacity at constant pressure (J kg^{-1} K^{-1})	730	700	550
Young's modulus (GPa)	70	140	1.5
Thermal expansion coefficient (10^{-6} K)	0.5	$\alpha(T)$	3

the same Peltier heater used for the conductive heating experiments. Red laser pulses (λ = 650 nm), normal to the testing chip, with duration of 0.5 s were used for photothermal actuation. The red laser beam was focused to ~600 μm in diameter in order to illuminate the entire cantilever during each pulse. Figure 2b shows the deflection measured as a function of laser pulse intensity. As shown in Figure 2c, all cantilevers have initial bending at 30 °C due to residual stress during fabrication. The actual intensity on the cantilever depends on the device bending angle, which means that it varies along its length. Furthermore, the bending angle changes during photothermal actuation, which makes the actual irradiance also a function of time through the actuation cycle. Thus, the laser intensities given were estimated by using the laser power and approximating the laser spot as a circle with a 600 μm in diameter.

It is noticed that, as shown in Figure 2b, the light intensity required to achieve the transition for each cantilever is different: the SWNT/VO_2-based actuator curve is shifted to the left. Only 1.8 × 10^4 mW/cm^2 is needed to initiate the phase transition in the SWNT/VO_2-based actuator, while about 2.9 × 10^4 mW/cm^2 is needed for the bare VO_2-based actuator. This represents 38% improvement of optical energy consumption. Similarly, the light intensity for full actuation of the SWNT/VO_2- and VO_2-based actuators are ~3.8 × 10^4 and ~6.0 × 10^4 mW/cm^2, respectively. It should also be mentioned that the intensity on the bare VO_2 device is actually larger than that on the SWNT/VO_2-based during the entire actuation range, since the initial curvature at room temperature for the former is smaller. Yet, the bare VO_2-based cantilever still requires larger laser intensity for reaching the phase transition. This supports the obervation of a lower intensity requirement for the SWNT/VO_2-based actuators. This improvement in energy consumption for the SWNT/VO_2-based device is attributed to a combination of the larger thickness and higher absorption of SWNT films (when compared to VO_2). However, although a larger thickness will improve absorption (at least up to a couple of SWNT skin depths), adding thickness to the actuator will increase its rigidity, and therefore could deteriorate the device performance.

The difference of the maximum deflections from uniform conductive heating and photothermal heating is due to the fact that in the photothermally actuated device part of the heat converted from light is dissipated through the cantilever's anchor, where the temperature is maintained at 30 °C; while in conductive heating there is very little difference in temperature between the cantilever, its anchor, and the substrate. Also, the uniform heating of the

cantilever when using conductive heating results in a uniform bending along its length, and thus a larger total deflection than when localized optical radiation is used for actuation. Thus, it should be clarified that a direct correlation between laser intensity and temperature using Figure 2a,b cannot be made, since the temperature boundary conditions for the lumped models of both mechanisms are not the same.

Another difference between two curves in Figure 2b is the slope during the transition, which represents the responsivity of the device. The results indicate that given the same change in laser intensity, the SWNT/VO_2-based actuator will produce a larger deflection (~3.84 μm/(mW·cm^{-2}) for the SWNT/VO_2-based and ~2.83 μm/(mW·cm^{-2}) for the bare VO_2-based). This is likely to be due to the combination of two mechanisms: the larger absorption of the SWNT film and the low thermal conductivity of SWNT films. This larger responsivity could also be beneficial if the presented devices were going to be used as light sensors.

The second part of the videos included in the Supporting Information show the deflection of both devices as 85 mW laser pulses are applied. These 85 mW laser pulses correspond to a light intensity of 2.9×10^4 mW/cm^2 (labeled in Figure 2b). The laser pulses in the video were 0.5 s long.

Measurement of Dynamic Performance. The optical actuation experiments demonstrated that the SWNT thin film significantly improved the efficiency and responsivity of the VO_2-based photoactuators. However, the effect of the SWNT layer on the dynamic performance of the VO_2-based photoactuators in terms of bandwidth was still unclear. Therefore, measurements of time response for the SWNT/VO_2- and bare VO_2-based actuators were performed by using a high speed camera (Nikon One J1 with 1200 frames per second). The results are shown in Figure 3. The laser pulse durations for both plots (Figure 3a,b) are 20 ms, but light intensities are different (labeled in Figure 2b as the green and red dashed lines). The light intensity used for Figure 3a is large enough to enter the phase transition for both devices. It can be seen how the displacement in both devices gradually decreases initially (outside the phase transition region) and then suddenly increases (as soon as the transition is reached), following the same behavior observed in Figure 2b. The faster response of the SWNT/VO_2-based actuator can be clearly noticed. The time constants for the SWNT/VO_2- and bare VO_2-based actuators were defined as the time from the start of the laser pulse to the steady state deflection value of the actuator. These time constants were measured during heating (see Figure 3a), which was slower than the cooling process for both devices, and their estimated values were 3.3 and 8.3 ms, respectively.

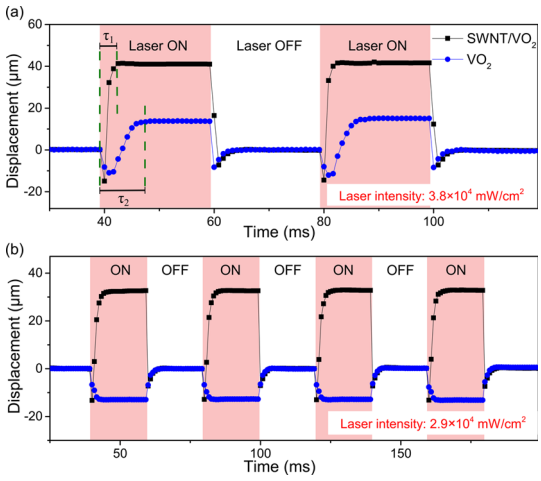

Figure 3. Measured time response of the VO_2 cantilevers and SWNT/VO_2-based cantilevers with driven laser intensity of (a) 3.8×10^4 mW/cm^2 and (b) 2.9×10^4 mW/cm^2. The duration of tested laser pulses is 20 ms.

If a slightly lower laser intensity is used (green dashed line in Figure 2b), the actuation of the SWNT/VO_2-based actuator still crosses most of the phase transition (see Figure 2b), but the VO_2-only device does not even reach the beginning of the phase transition, thereby exhibiting only downward displacement (Figure 3b).

Light Absorption Efficiency Calculation. To help analyze the obtained results and quantify the increase in light absorption efficiency, a numerical simulation using finite element method (FEM) implemented with COMSOL software was conducted. The results are summarized in Figure 4. The study in COMSOL used a steady-state heat transfer and solid mechanics modules with the three-dimensional geometry of the cantilever presented in this work. The heat converted from the laser was simulated by an inflow heat flux boundary condition on the top cantilever surface with controlled intensity. The effects of heat transfer through the surrounding air (convection losses) were also included in the simulations. Thermal radiation losses were neglected. Commonly accepted values were used for SiO_2 thermal properties, and the properties for VO_2, and SWNTs used in the simulation were taken from the literature,[24,35,37−39] and are summarized in Table 1. The thermal expansion coefficient of VO_2 was assumed as a function of temperature to simulate the phase transition of VO_2 (as it was done in Cabrera *et.al*[24]). The values for $\alpha(T)$ in Table 1 were in the range of $2.3-5 \times 10^{-6}$/K.

Due to the heat sink function of the anchor, and convection cooling of the air, the temperature distribution along the device is not uniform when uniform heat influx is applied. The temperature distribution along the SWNT/VO_2-based cantilever is shown in Figure 4a with a heat flux of 6.7×10^3 mW/cm^2. From the simulations, the necessary intensity of heat flux to

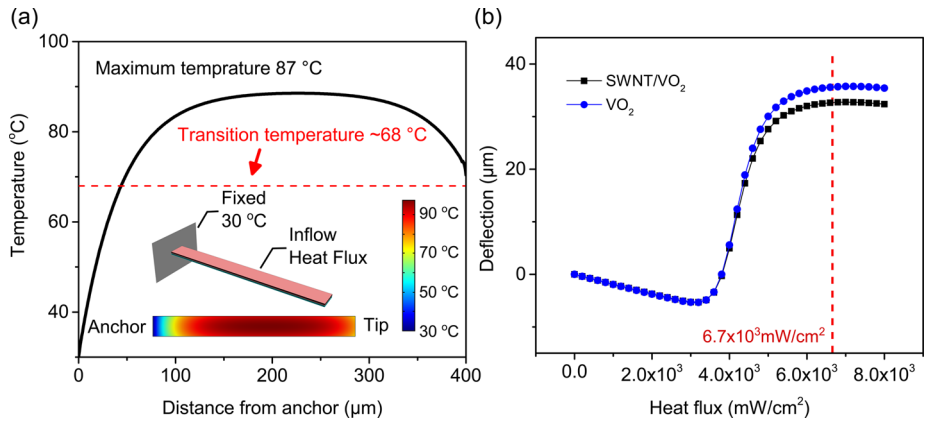

Figure 4. (a) Calculated temperature distribution along the SWNT/VO_2-based cantilever with heat flux intensity of 6.7 × 10^3 mW/cm^2. The red dash line represents the transition temperature. (b) Calculated deflection of cantilevers as a function of heat flux.

reach maximum deflection was estimated to be 6.7 × 10^3 mW/cm^2 for the SWNT/VO_2- and bare VO_2-based actuators (see Figure 4b). With the use of the estimated laser intensities for full actuation for both devices mentioned earlier (and shown in Figure 2b) and the simulation, the transfer efficiencies from optical energy to heat can be calculated to be 17.6% and 11.7% for the SWNT/VO_2- and bare VO_2-based devices, respectively.

TABLE 2. Performance Comparison between Both Presented Devices

performance	VO_2-based	SWNT/VO_2-based
Laser intensity for full actuation (mW/cm^2)	~6.0 × 10^4	~3.8 × 10^4
Absorption efficiency (%)	11.7	17.6
Responsivity (μm/mW-cm^{-2})	2.83	3.84
Time constant (ms)	8.3	3.3

CONCLUSION

In summary, a new and simple approach to increase the efficiency, responsivity, and speed of VO_2-based photothermally driven actuators is presented, which utilizes the excellent light-absorbing properties of a SWNT film prepared using a simple vacuum filtration process. Table 2 summarizes the comparison between the two presented devices. The improvements are mainly attributed to the better optical absorption, larger thickness, and lower thermal conductivity of SWNT films, when compared to VO_2 films. The transferring of the SWNT did not alter the VO_2 film quality, which represents an opportunity to further expand the integration of SWNTs and VO_2 films to a plurality of device designs and applications. Moving forward, the SWNT/VO_2 photoactuators can be optimized in terms of SWNT and VO_2 thickness. Moreover, by using purified SWNTs with different chirality distribution and thereby different absorption spectra, programmable wavelength-selective photoactuator can be obtained.

METHODS

VO_2 Deposition. VO_2 thin film was deposited, through pulsed laser deposition, on the SiO_2 thin layer. The substrate was placed into a vacuum chamber with oxygen gas pressure at 20 mTorr. A metallic vanadium target, 2 in. apart from the sample, was ablated by excimer laser pulses with energy of 352 mJ per pulse (fluence of ~2 J/cm^2) and a frequency of 10 Hz. A ceramic heater used to heat the sample was maintained at 595 °C through 25 min deposition. Following the deposition, 30 min annealing process was performed with the same deposition conditions. To determine the quality of the VO_2 film, the resistance of the VO_2 film was measured as a function of temperature which cycled from 30 to 100 °C. The resistance measurement of VO_2 thin film shows approximately 2 orders in magnitude drop in film resistance, which indicates good quality of VO_2.

SWNT Thin-film Fabrication and Transfer. The SWNT thin-film fabrication follows, in general, the same processes described in the literature.[35] A 0.1 mg/mL SWNT solution was made of purified SWNT powder purchased from Cheap Tube, Inc. (Purity >99 wt %, diameter 0.8−1.6 nm, length 3−30 m), and mixed with 2% sodium deoxycholate as surfactant. A 400 min sonication (Crest Ultrasonic) was performed to completely dissolve the SWNT powder, followed by 10 min centrifugation with 13 000 rpm rotation speed, which removed large SWNT aggregates and non-SWNT impurities. Vacuum filtration was then used to fabricate SWNT thin film on cellulose membranes from SWNT solution. The thickness of SWNT thin film can be precisely controlled by adjusting the concentration and the amount of solution used for filtration. To obtain good adhesion between SWNT and VO_2, surface functionalization was performed by immersing the target substrate into poly-L-lysine solution for 5 min. The cellulose/SWNT membrane was attached to VO_2 surface of target substrate with SWNT side facing toward the substrate. Several drops of deionized (DI) water were used to keep the membrane at the desired position. Then, the substrate was placed up-side-down in a beaker containing acetone on a hot plate set to 70 °C. After about 30 min acetone vapor bath, the cellulose membrane was dissolved, leaving only SWNT film on the substrate. The transfer process was completed by briefly rinsing the sample with acetone, isopropanol, and then blowing dry.

Deflection Measurement. The tested samples were installed on top of a Peltier heater attached on a micrometer translation stage. Above the sample, a red laser (650 nm) focused by a lens was used to illuminate photoactuators. A camera placed at one side is responsible for imaging and recording the cantilever

during actuation. Software Tracker tracked the tip movement of cantilever in the video, and the length of the cantilever (400 μm) was used to calibrate the deflection.

Conflict of Interest: The authors declare no competing financial interest.

Acknowledgment. This work was partially supported by the National Science Foundation under Grant ECCS 1306311; and by the American Society for Engineering Education (ASEE) through a summer faculty fellowship program. The authors would like to thank Prof. Junghoon Yeom for helpful discussions regarding SWNT film transfer.

Supporting Information Available: Videos showing deflection of both devices as the heater temperature is increased from 30 to 100 °C and as 85 mW laser pulses are applied (.mpg) and explanations of videos. This material is available free of charge *via* the Internet at http://pubs.acs.org.

REFERENCES AND NOTES

1. Morin, F. J. Oxides Which Show a Metal-to-Insulator Transition at the Neel Temperature. *Phys. Rev. Lett.* **1959**, *3*, 34–36.
2. Imada, M.; Fujimori, A.; Tokura, Y. Metal-Insulator Transitions. *Rev. Mod. Phys.* **1998**, *70*, 1039–1263.
3. Haverkort, M. W.; Hu, Z.; Tanaka, A.; Reichelt, W.; Streltsov, S. V.; Korotin, M. A.; Anisimov, V. I.; Hsieh, H. H.; Lin, H.-J.; Chen, C. T.; et al. Orbital-Assisted Metal-Insulator Transition in VO_2. *Phys. Rev. Lett.* **2005**, *95*, 196404−1–196404−4.
4. Lysenko, S.; Vikhnin, V.; Zhang, G.; Rua, A.; Fernández, F. E.; Liu, H. Insulator-to-Metal Phase Transformation of VO_2 Films upon Femtosecond Laser Excitation. *J. Electron. Mater.* **2006**, *35*, 1866–1872.
5. Hu, B.; Ding, Y.; Chen, W.; Kulkarni, D.; Shen, Y.; Tsukruk, V. V.; Wang, Z. L. External-Strain Induced Insulating Phase Transition in VO_2 Nanobeam and Its Application as Flexible Strain Sensor. *Adv. Mater.* **2010**, *22*, 5134–5139.
6. Ko, C.; Ramanathan, S. Observation of Electric Field-Assisted Phase Transition in Thin Film Vanadium Oxide in a Metal-Oxide-Semiconductor Device Geometry. *Appl. Phys. Lett.* **2008**, *93*, 252101−1–252101−3.
7. Barker, A. S.; Verleur, H. W.; Guggenheim, H. J. Infrared Optical Properties of Vanadium Dioxide Above and Below the Transition Temperature. *Phys. Rev. Lett.* **1966**, *17*, 1286–1289.
8. Verleur, H. W.; Barker, A. S.; Berglund, C. N. Optical Properties of VO_2 between 0.25 and 5 eV. *Phys. Rev.* **1968**, *172*, 788–798.
9. Mott, N. F.; Friedman, L. Metal-Insulator Transitions in VO_2, Ti_2O_3 and $Ti_{2-x}V_xO_3$. *Philos. Mag.* **1974**, *30*, 389–402.
10. Stefanovich, G.; Pergament, A.; Stefanovich, D. Electrical Switching and Mott Transition in VO_2. *J. Phys.: Condens. Matter.* **2000**, *12*, 8837–8845.
11. Cavalleri, A.; Dekorsy, T.; Chong, H. H. W.; Kieffer, J. C.; Schoenlein, R. W. Evidence for a Structurally-Driven Insulator-to-Metal Transition in VO_2: A View from the Ultrafast Timescale. *Phys. Rev. B* **2004**, *70*, 161102−1–161102−4.
12. Rúa, A.; Fernández, F. E.; Sepúlveda, N. Bending in VO_2-Coated Microcantilevers Suitable for Thermally Activated Actuators. *J. Appl. Phys.* **2010**, *107*, 074506-1–074506-4.
13. Cao, J.; Fan, W.; Zhou, Q.; Sheu, E.; Liu, A.; Barrett, C.; Wu, J. Colossal Thermal-mechanical Actuation *via* Phase Transition in Single-Crystal VO_2 Microcantilevers. *J. Appl. Phys.* **2010**, *108*, 083538−1–083538−4.
14. Cabrera, R.; Merced, E.; Sepúlveda, N. A Micro-Electro-Mechanical Memory Based on the Structural Phase Transition of VO_2. *Phys. Status Solidi A* **2013**, *210*, 1704–1711.
15. Davila, N.; Merced, E.; Sepúlveda, N. Electronically Variable Optical Attenuator Enabled by Self-Sensing in Vanadium Dioxide. *IEEE Photonics Technol. Lett.* **2014**, *26*, 1011–1014.
16. Ha, S.; Zhou, Y.; Duwel, A.; White, D.; Ramanathan, S. Quick Switch: Strongly Correlated Electronic Phase Transition Systems for Cutting-Edge Microwave Devices. *IEEE Microwave Mag.* **2014**, *15*, 32–44.
17. Merced, E.; Tan, X.; Sepúlveda, N. Strain Energy Density of VO_2-Based Microactuators. *Sens. Actuators, A* **2013**, *196*, 30–37.
18. Liu, K.; Cheng, C.; Cheng, Z.; Wang, K.; Ramesh, R.; Wu, J. Giant-Amplitude, High-Work Density Microactuators with Phase Transition Activated Nanolayer Bimorphs. *Nano Lett.* **2012**, *12*, 6302–6308.
19. Lee, S.; Cheng, C.; Guo, H.; Hippalgaonkar, K.; Wang, K.; Suh, J.; Liu, K.; Wu, J. Axially Engineered Metal-Insulator Phase Transition by Graded Doping VO_2 Nanowires. *J. Am. Chem. Soc.* **2013**, *135*, 4850–4855.
20. Tselev, A.; Budai, J. D.; Strelcov, E.; Tischler, J. Z.; Kolmakov, A.; Kalinin, S. V. Electromechanical Actuation and Current-Induced Metastable States in Suspended Single-Crystalline VO_2 Nanoplatelets. *Nano Lett.* **2011**, *11*, 3065–3073.
21. Pellegrino, L.; Manca, N.; Kanki, T.; Tanaka, H.; Biasotti, M.; Bellingeri, E.; Siri, A. S.; Marré, D. Multistate Memory Devices Based on Free-standing VO_2/TiO_2 Microstructures Driven by Joule Self-Heating. *Adv. Mater.* **2012**, *24*, 2929–2934.
22. Bae, S.-H.; Lee, S.; Koo, H.; Lin, L.; Jo, B. H.; Park, C.; Wang, Z. L. The Memristive Properties of a Single VO_2 Nanowire with Switching Controlled by Self-Heating. *Adv. Mater.* **2013**, *25*, 5098–5103.
23. Coy, H.; Cabrera, R.; Sepúlveda, N.; Fernández, F. E. Optoelectronic and All-Optical Multiple Memory States in Vanadium Dioxide. *J. Appl. Phys.* **2010**, *108*, 113115−1–113115−6.
24. Cabrera, R.; Merced, E.; Sepúlveda, N. Performance of Electro-Thermally Driven VO_2-Based MEMS Actuators. *J. Microelectromech. Syst.* **2014**, *23*, 243–251.
25. Najar, F.; Choura, S.; El-Borgi, S.; Abdel-Rahman, E. M.; Nayfeh, A. H. Modeling and Design of Variable-Geometry Electrostatic Microactuators. *J. Micromech. Microeng.* **2005**, *15*, 419–429.
26. Adriaens, H.; De Koning, W.; Banning, R. Modeling Piezoelectric Actuators. *IEEE/ASME Trans. Mechatronics* **2000**, *5*, 331–341.
27. Que, L.; Park, J.-S.; Gianchandani, Y. Bent-Beam Electro-Thermal Actuators for High Force Applications. *IEEE Int. Conf. Micro Electro Mech. Syst., 12th* **1999**, 31–36.
28. Que, L.; Park, J.-S.; Gianchandani, Y. Bent-Beam Electrothermal Actuators-Part I: Single Beam and Cascaded Devices. *J. Microelectromech. Syst.* **2001**, *10*, 247–254.
29. Que, L.; Park, J.-S.; Li, M.-H.; Gianchandani, Y. Reliability Studies of Bent-Beam Electro-thermal Actuators. *Annu. Proc.—Reliab. Phys. [Symp.]* **2000**, 118–122.
30. Luo, J.; Fu, Y.; Williams, J.; Milne, W. Thermal Degradation of Electroplated Nickel Thermal Microactuators. *J. Microelectromech. Syst.* **2009**, *18*, 1279–1287.
31. Zhao, Y.; Karaoglan-Bebek, G.; Pan, X.; Holtz, M.; Bernussi, A. A.; Fan, Z. Hydrogen-Doping Stabilized Metallic VO_2 (R) Thin Films and Their Application to Suppress Fabry-Perot Resonances in the Terahertz Regime. *Appl. Phys. Lett.* **2014**, *104*, 241901-1–241901-5.
32. Mlyuka, N. R.; Niklasson, G. A.; Granqvist, C. G. Mg Doping of Thermochromic VO_2 Films Enhances the Optical Transmittance and Decreases the Metal-Insulator Transition Temperature. *Appl. Phys. Lett.* **2009**, *95*, 171909-1–171909-3.
33. Zhao, Y.; Hwan Lee, J.; Zhu, Y.; Nazari, M.; Chen, C.; Wang, H.; Bernussi, A.; Holtz, M.; Fan, Z. Structural, Electrical, and Terahertz Transmission Properties of VO_2 Thin Films Grown on c-, r-, and m-Plane Sapphire Substrates. *J. Appl. Phys.* **2012**, *111*, 053533-1–053533-8.
34. Li, J.; Dho, J. Characteristics of Phase Transition of VO_2 Films Grown on TiO_2 Substrates with Different Crystal Orientations. *J. Cryst. Growth* **2014**, *404*, 84–88.
35. Zhang, X.; Yu, Z.; Wang, C.; Zarrouk, D.; Seo, J.-W. T.; Cheng, J. C.; Buchan, A. D.; Takei, K.; Zhao, Y.; Ager, J. W.; et al. Photoactuators and Motors Based on Carbon Nanotubes with Selective Chirality Distributions. *Nat. Commun.* **2014**, *5*, 2983-1–2983-8.

36. Kataura, H.; Kumazawa, Y.; Maniwa, Y.; Umezu, I.; Suzuki, S.; Ohtsuka, Y.; Achiba, Y. Optical Properties of Single-Wall Carbon Nanotubes. *Synth. Met.* **1999**, *103*, 2555–2558.
37. Tsai, K.-Y.; Chin, T.-S.; Shieh, H.-P. D. Effect of Grain Curvature on Nano-Indentation Measurements of Thin Films. *Jpn. J. Appl. Phys.* **2004**, *43*, 6268–6273.
38. Berglund, C. N.; Guggenheim, H. J. Electronic Properties of VO_2 near the Semiconductor-Metal Transition. *Phys. Rev.* **1969**, *185*, 1022–1033.
39. Oh, D.-W.; Ko, C.; Ramanathan, S.; Cahill, D. G. Thermal Conductivity and Dynamic Heat Capacity Across the Metal-Insulator Transition in Thin Film VO_2. *Appl. Phys. Lett.* **2010**, *96*, 151906−1–151906−3.